Hindawi
Scientific Programming
Volume 2022, Article ID 7129775, 10 pages
https://doi.org/10.1155/2022/7129775

Research Article

Design of Investment Potential Analysis Model of Integrated Energy Project Based on Deep Learning Neural Network

Rifu Huang[1], **Tianyao Xu**[1], **Chenkai Fan**[1], **Xiaoyong Hu**[1], **Wanyue Xu**[1], **Panfei Li**[1], **Kailing Lu**[1], **Wei Liu**[2], **Yakai Zhang**[2], **Peitao Li**[2], and **V.T. Pham**[3]

[1]*China Three Gorges Corporation, Wuhan 430010, Hubei, China*
[2]*Tianjin Tianda Qiushi Power New Technology Co., Ltd., Tianjin 300384, China*
[3]*Saigon University, Ho Chi Minh City, Vietnam*

Correspondence should be addressed to Rifu Huang; huang_rifu@ctg.com.cn

Received 20 April 2022; Revised 26 May 2022; Accepted 30 May 2022; Published 25 June 2022

Academic Editor: Lianhui Li

Under the background of energy conservation and emission reduction and large-scale promotion of electric energy substitution, fully exploring the complementary potential of various energy systems and realizing the optimization of comprehensive energy utilization are the most critical development goals of the current energy system. The key to achieving this goal is the investment potential analysis of integrated energy projects. In order to effectively solve the problems of difficult scientific determination of evaluation index weight and low accuracy of evaluation results in the analysis of investment potential of integrated energy projects, an investment potential analysis model of integrated energy project based on deep learning neural network is designed. The design process of the integrated energy project is summarized. The RBF-BP neural network model is established to obtain the correlation between the factors of the evaluation unit, further analyze and process the training results, and calculate the weight of the evaluation index. The obtained weight is substituted into the TOPSIS comprehensive evaluation model for the investment potential analysis of integrated energy projects. According to the investment potential analysis results, the investment potential analysis value of energy performance contracting (EPC) mode is 0.9122, which is the best operation mode. The results show that the analysis results reflect the investment potential of integrated energy projects more objectively and scientifically.

1. Introduction

Integrated energy system includes the production, use, and transmission of different types of energy, including many conventional energy subsystems, such as natural gas system and traditional power system, as well as new energy generation systems, such as geothermal power generation and wind power generation [1–5]. The integrated energy system can realize the comprehensive utilization of different types of energy, reduce the problems in energy supply, reduce the number of energy conversion, and reduce environmental pollution. It can not only meet people's demand for electricity, but also realize many other services, such as refrigeration and heating, so as to realize the cascade use of energy; improve energy efficiency; and promote the sustainable development of society, market economy, and energy [4]. However, there are many subsystems in the integrated energy system, and the operation mode and functional characteristics of these subsystems are also very different. The integrated energy system has rich levels, diversified structures, and nonlinear and multiple space-time characteristics, in which there are many problems to be solved. It is difficult to solve the problems only by using the traditional operation mode, control technology, and modeling and simulation technology [5].

The premise of investment potential analysis of integrated energy system is to realize system integration and optimization [6, 7]. The feasibility study, design, and operation mode optimization of integrated energy project need to be carried out on the basis of investment potential analysis. Therefore, the importance of investment potential analysis of integrated energy projects is extraordinary.

With the development of information technology [7–11], artificial intelligence technology has been gradually applied in various industries [12–16]. Because BP neural network [17–19] has strong learning ability and nonlinear fitting ability; it has been empirically applied to the field of investment potential analysis of integrated energy projects. In this paper, RBF-BP neural network is proposed and used to calculate the weight of investment potential evaluation index of integrated energy project. The example shows that this method not only makes full use of the advantages of fast approximation speed of RBF neural network, but also has the ability of BP neural network to better predict unknown samples and improve the evaluation accuracy.

The rest of this article is organized as follows. Section 1 introduces the engineering design of integrated energy project. The principle and algorithm design of RBF-BP neural network are described in Section 2. In Section 3, construction of index system and evaluation index weight solution based on RBF-BP neural network model are applied in a case, and finally the investment potential analysis result is obtained. The main contributions of this study are summarized and analyzed in Section 4.

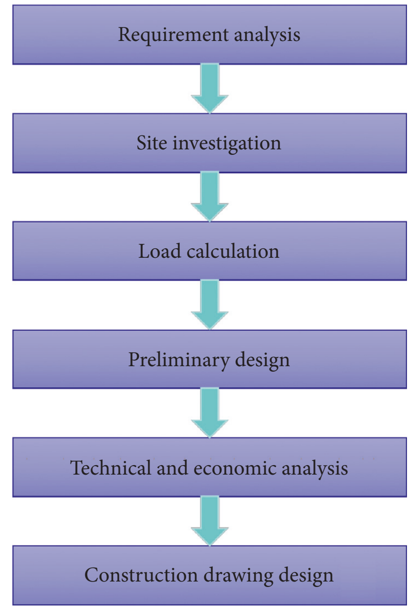

Figure 1: Technical scheme design process of integrated energy projects.

2. Engineering Design of Integrated Energy Project

According to different energy demands, integrated energy projects can be divided into solar energy and heat pump collaborative heating scheme; solar energy and low valley electric heat storage collaborative heating scheme; heat pump and low valley electric heat storage collaborative heating scheme; solar energy, heat pump, and low valley electric heat storage collaborative heating scheme. The collaborative controller is used to realize the collaborative regulation of different technologies. The standard of collaborative control is generally that the heat pump supplies the basic heat load. In the area with sufficient light, the solar heat collection is large, and the heat pump load is appropriately reduced. In areas with preferential valley price, electric boilers can be used to store heat in the valley to reduce the load of heat pump. Through the analysis and comparison of the investment potential of different technical schemes, the project technical scheme suitable for the industrial park is selected.

As shown in Figure 1, the technical scheme design process of integrated energy projects is divided into five steps:

(1) Requirement analysis: heating load demand of users in heating season, including design heat load, average heat load, and minimum heat load; annual heat load continuation diagram and analysis; hourly heat load calculation; annual average heat load simulation calculation and analysis, etc.

(2) Site investigation: understand the building system characteristics, energy structure around the building, climate resources, and other conditions in detail, and judge the applicable technology on site.

(3) Preliminary design: according to the analysis of users' heat load characteristics, determine the proportion and supply period of solar hot water heating. Combined with the heating load borne by solar energy and its time period, analyze whether it has the spatial and economic conditions for the implementation of electric heat storage. Comparative analysis of heat pump collaborative heating schemes is applied, especially for users with large-scale and stable needs of heating and refrigeration.

(4) Technical and economic analysis: determine the technical scheme and conduct technical and economic review on the scheme.

(5) Construction drawing design: issue detailed construction drawing design, and provide the list of materials, equipment, and project budget.

The main functions of the integrated energy project include the following:

(1) *Energy Monitoring.* From the perspective of the safe and stable operation of the energy network, the production and operation of energy subsystems such as electricity, cold/hot water, hot water, important energy production equipment in the park, and the energy consumption of buildings in the park are monitored through the three-dimensional visualization platform, so as to ensure the stable and safe operation of the park.

(2) *Energy Regulation.* With the help of a variety of technologies to complete the interaction between user load demand and energy production, such as optimizing the ratio, different energy amounts can be fully utilized.

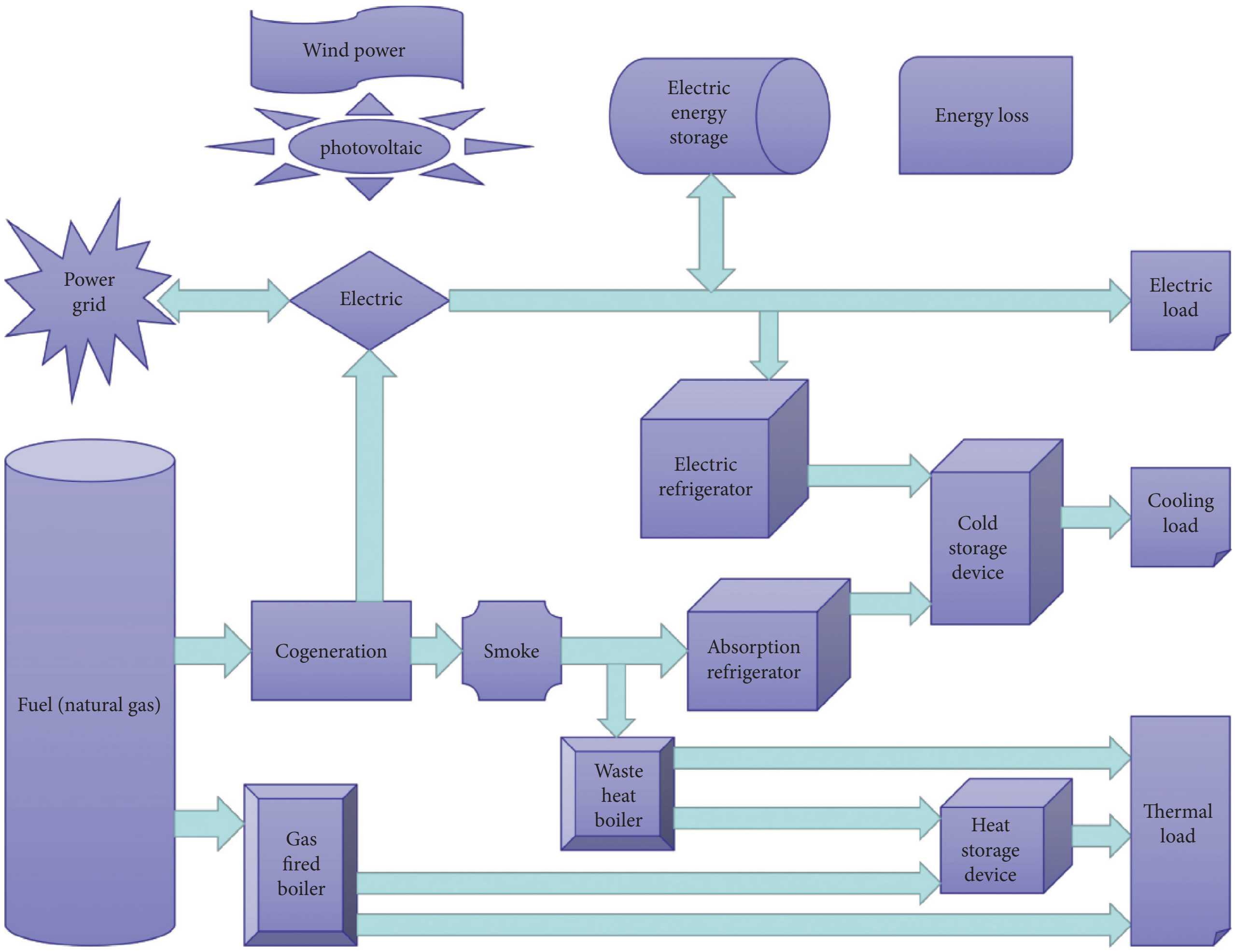

Figure 2: The energy flow of the integrated energy project.

(3) *Energy Analysis.* The interactive analysis of the power grid structure and the improvement of the power grid structure will provide the interactive support for the power grid decision-makers from the perspective of the visualization of the power grid structure and safety.

(4) *Asset Operation and Maintenance Management.* Through the management business of the whole life cycle of equipment in the park, intelligent patrol inspection business, digital maintenance business, and process three-line operation and maintenance business, realize the structured management, process standardization of the park, and provide information support for the information management of equipment inspection and maintenance in the park.

The energy flow of the integrated energy project is shown in Figure 2.

3. RBF-BP Neural Network Model

3.1. RBF and BP Neural Network Structure. BP neural network and RBF neural network are two commonly used neural network algorithms [20, 21]. As a global approximation network, BP neural network is a stable and reliable nonlinear function approximation method. However, it has the disadvantages of slow convergence speed and easy-to-trap local minimum, although the system is unstable and difficult to ensure that the learning result can reach the global minimum of mean square error. However, the system has good generalization performance. RBF neural network is a kind of optimal approximation network. If there are enough neurons in the hidden layer, it can approximate any continuous nonlinear function with arbitrary precision. RBF neural network has the advantages of simple training and fast learning convergence, overcoming local minimum problem, but having poor generalization ability. RBF-BP neural network combines the advantages of RBF neural network and BP neural network [20–26]. It consists of RBF subnet and BP subnet. Among them, a 4-layer neural network system includes input layer, two hidden layers, and output layer. The model structure is shown in Figure 3.

n, j, k, and m represent the number of neurons in input layer, first hidden layer, second hidden layer, and output layer, respectively. σ_j is the Gauss function width matrix. $C_{n,j}$ is the central vector matrix. $w_{k,j}$ is the weight matrix

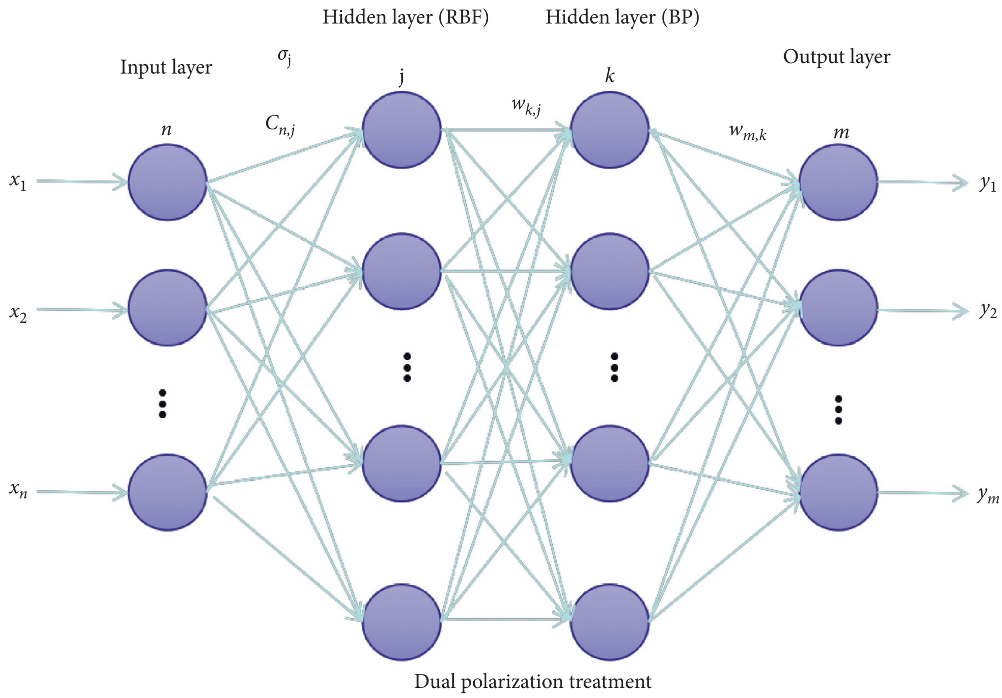

Figure 3: RBF-BP neural network structure.

between the second hidden layer and the second hidden layer. $w_{m,k}$ is the weight matrix between the second hidden layer and the output layer. The activation function of neurons in the first hidden layer is Gauss-type function. The activation function of neurons in the second hidden layer is Sigmoid-type function.

3.2. RBF and BP Neural Network Algorithm Design. According to the input training samples, through the RBF subnet preliminary training. After kernel mapping of the input sample by the hidden layer node of RBF subnet, the kernel mapping value needs to be double-polarized before it can be used as the input of BP network. The formula for $\varphi_j(x)$ dual polarization treatment is

$$\varphi_j(x) = 2.\varphi_j(x) - 1. \tag{1}$$

First the output of the hidden layer (i.e., input of BPNN) is as follows:

$$h_i = \sum_{j=1}^{N_2} w_{ij}\varphi_j(x),\ i = 1, 2, \cdots, N_3, \tag{2}$$

where N_3 is the number of nodes of the second hidden layer (BP) and w_{ij} is the weight between the two hidden layers.

Then, the output of RBF subnet is used as the input of BP subnet for strengthening training. Finally, BP subnet training results are obtained. It identifies and outputs results quantitatively. The algorithm flow is shown in Figure 4.

RBF and BP algorithm to realize the detailed steps are as follows.

Step 1. Initialize the weights and widths of each layer. Randomly set to the smaller number between [0,1]. Set parameters such as maximum training times, target accuracy, and learning rate.

Step 2. Calculate the center vector. Set the transfer function of RBF subnet hidden layer to Gauss function. It has the following form:

$$\varphi_j(x) = \exp\left(-\frac{x - C_j{}^2}{2b_j^2}\right), j = 1, 2, \cdots, N_3, \tag{3}$$

where φ is the output of RBF hidden layer node. N_2 is the number of nodes in the hidden layer. X is the input sample vector. C_j represents the center vector of the Gaussian kernel function. b_i represents the Gaussian kernel width of the JTH neuron ($b = d_{\max}/\sqrt{2N_2}$, $d_{\max}$ is the maximum value of each cluster center). $x - C_j$ is the Euclidean distance between x and C_j.

Step 3. Set the transfer function of BP subnet hidden layer as Sigmoid-type function:

$$F(h_i) = \frac{1}{1 + \exp(-h_i)}, i = 1, 2, \cdots, N_3. \tag{4}$$

Step 4. Calculate the output value of node M at the output layer. Linear transfer function is adopted, which is expressed as

$$y(m) = \sum_{l=1}^{N_3} w_{lm}F(h_i), m = 1, 2, \cdots, N_4, \tag{5}$$

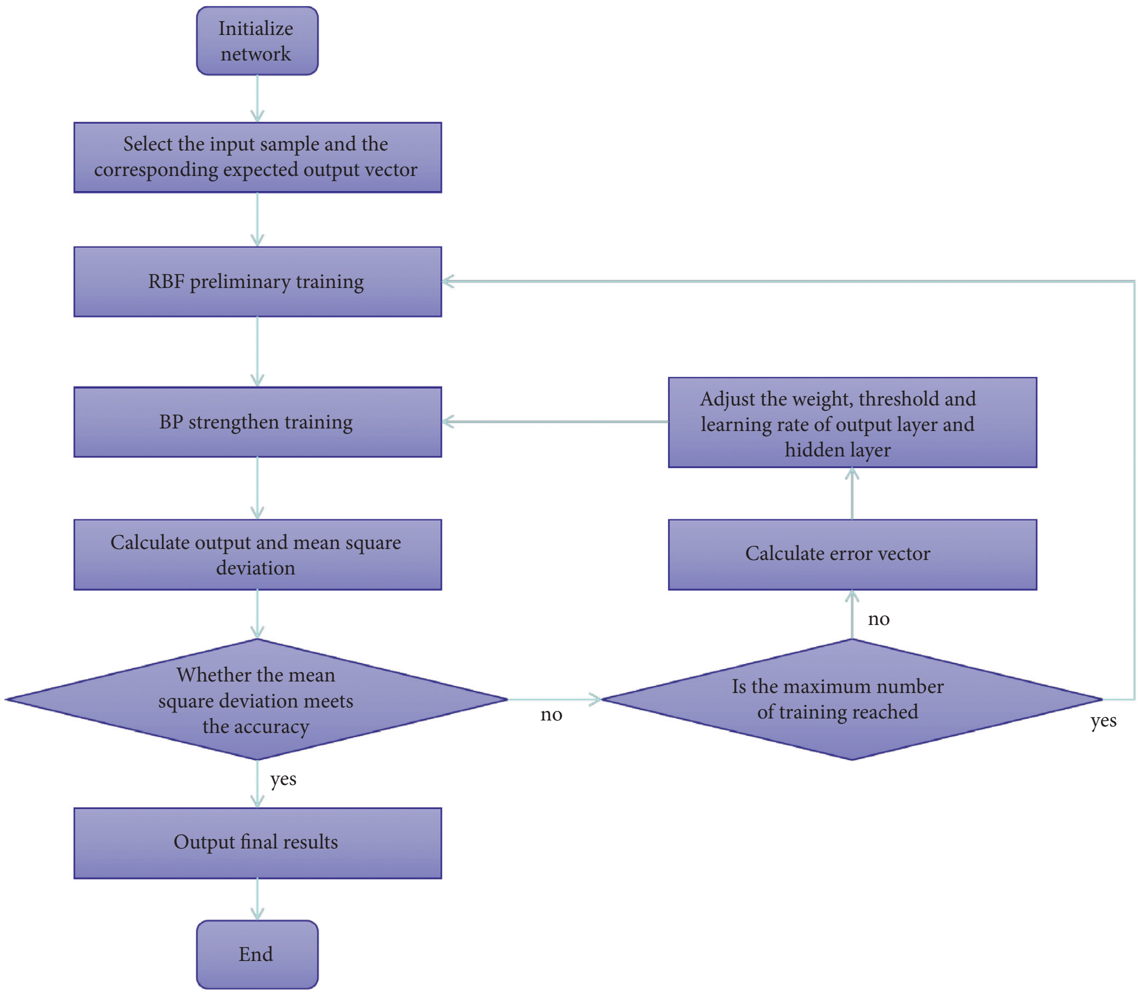

Figure 4: Algorithm flow.

where $y(m)$ is the output value of the m-th node in the output layer. N_4 indicates the number of output layers. w_{lm} represents the connection weight between neuron l of the full hidden layer and neuron m of the output layer.

$$E = \sum_{k=1}^{N_4} [d_k - y(m)]^2, \tag{6}$$

where d_k is the expected output value.

Step 6. Calculate the error vector of each neuron in the output layer:

$$\mathrm{ERR}_m = y(m)[1 - y(m)][d_k - y(m)]^2. \tag{7}$$

Step 7. Adjust the weight of each layer, rich value vector.

The weight coefficient w is adjusted according to the difference between the known output data d_j and the output data $y(j)$ calculated by formula (5). The formula of adjustment quantity is

$$\Delta w_{ij} = \eta \delta_j x_j, \tag{8}$$

where η is the learning rate (proportional coefficient) that can be adjusted adaptively. It is set to a value between [0,1] in the calculation. In network training, the value can be gradually increased until the satisfactory training speed can be achieved if the oscillation cannot be caused and the high precision can be ensured. x_j at the hidden node is the input of the whole network. In the output node, it is the output of the lower level (hidden layer) node ($j = 1, 2, \cdots, N_4$). δ_j is a value associated with output bias. For the output node,

$$\delta_j = \eta(1 - y(j))\big(d_j - y(j)\big). \tag{9}$$

For hidden layer nodes, the outputs are not comparable. Therefore, after reverse calculation, there are

$$\delta_j = x_j\big(1 - x_j\big)\sum_k \delta_k w_{jk}, \tag{10}$$

where k refers to traversing the upper (output layer) node. Error δ_j is calculated from the output layer backward layer by layer.

Each layer neuron weight is adjusted for

$$w_{ij}(t) = w_{ij}(t-1) + \Delta w_{ij}, \tag{11}$$

where t is the learning times. Each layer neuron weight is adjusted for

$$\theta_j = \theta_j + \eta.\mathrm{ERR}_j, \tag{12}$$

where η represents the learning rate.

In the process of running the program, when the training error of RBF-BP neural network is less than the set target accuracy, the training ends. At this point, it is converging. If the number of training selection times is greater than the maximum number of training times, it has not reached the target precision and the network structure does not converge. It returns to Step 2 and continues executing the program until the process converges.

4. Case Study

According to the field investigation and cooperation negotiation, there are three operation modes that can be applied to the comprehensive energy project in an industrial park: EPC mode, construction operation transfer (BOT) mode, and public-private partnership (PPP) mode. This section will build a comprehensive evaluation index system of investment potential of comprehensive energy department projects, use the model in Section 2 to solve the index weight, analyze the investment potential, and select the most suitable operation mode.

4.1. Construction of Index System. The key to the optimal planning and design of integrated energy service system is to determine the type and composition of equipment with long-term economy, energy conservation, and environmental protection according to the total cold, heat, and power demand of regional users and build a high-energy efficiency system. The construction of integrated evaluation index system is shown in Table 1.

Table 1: Integrated evaluation index system.

Index type	Index name
Economy feature	Annual comprehensive energy efficiency
Economy feature	Electricity charge savings
Energy saving feature	Total primary energy consumption
Energy saving feature	Annual electric energy substitution
Environmental protection feature	CO_2 emission reduction
Environmental protection feature	SO_2 emission reduction
Environmental protection feature	NO_x emission reduction

4.2. Evaluation Index Weight Solution Based on the RBF-BP Neural Network Model

4.2.1. Comprehensive Evaluation Model. In order to explain the investment potential level of an integrated energy project, the contribution and influence of the single factors in the above studies on the investment potential of integrated energy project are different. The contribution degree of each evaluation factor to the investment potential of integrated energy project in an industrial park was calculated by RBF-BP neural network. The calculation is as follows:

$$CI_i = \sum_{j=1}^{n} I_i w_{ij}, \tag{13}$$

where $I\ j$ is the j-th evaluation factor and w_{ij} is the weight of the j-th evaluation factor.

4.2.2. RBF and BP Neural Network Model Structure Determination. In order to obtain the weight of each evaluation index, it is necessary to standardize the value of the evaluation index. The reverse index and moderate index also need to do forward processing. This makes the values of all evaluation indicators between [0,1]. Positive indicators are standardized by maximum effect method (equation (14)). The minimum effect method is adopted to realize standardization of backward indicators (equation (15)). Moderate indicators are standardized by central effect method (equation (16)):

$$x_i' = 100 \times \frac{x_i - x_{\min}}{x_{\max} - x_{\min}}, \tag{14}$$

$$x_i' = 100 \times \frac{x_{\max} - x_i}{x_{\max} - x_{\min}}, \tag{15}$$

$$x_i' = \begin{cases} 100 \times \dfrac{x_i - x_{\min}}{k - x_{\min}}, x_i < k, \\ 100 \times \dfrac{x_{\max} - x_i}{x_{\max} - k}, x_i > k, \end{cases} \tag{16}$$

where x_i represents the actual value of the i-th lattice of this indicator. x_i' represents the forward normalized value. k is the most moderate value of this factor.

After standardized treatment, there is no difference in dimension, order of magnitude, and degree of variation among factors. Then, RBF-BP neural network model was used to solve the weight of each single factor.

Firstly, the number of neurons in each layer of RBF-BP neural network was determined, since the weight of four individual indicators was required in this study. Then, the number of input layer and output neural unit is set to 4. Forty groups of data were selected as training samples of neural network. Ten groups of data were used as test samples. Through continuous debugging, if the number of input layer neurons <the number of neurons in the hidden layer ≤ the principle of number of neurons in input layer + number of neurons in output layer, the number of neurons in the first hidden layer and the second hidden layer is set to 5. The network structure is shown in Figure 5.

The activation function of the first hidden layer adopts radbas( ) function. The activation function of the second hidden layer is tangent S-type transfer function tansig( ). The neuron transfer function of the output layer adopts the linear transfer function purelin( ). Network training algorithm uses

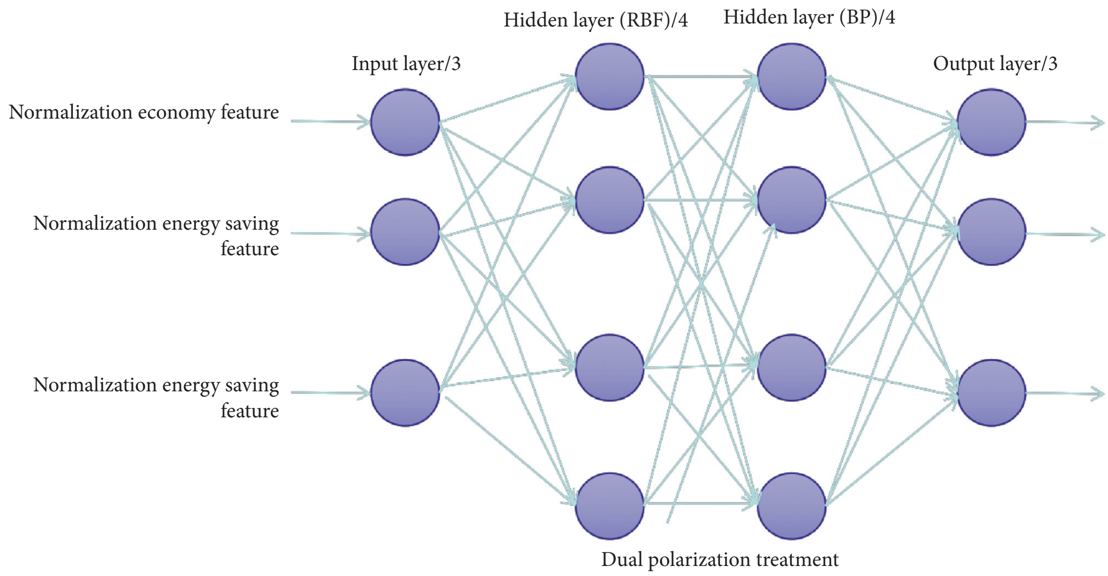

Figure 5: Network structure.

LM algorithm trainlm( ). Learning function uses gradient descent momentum learning function Learngdm( ).

We apply newff() to construct rBF-BP network: Net = newff(minmax(C), [S, 4, 4], {'radbas', 'tansig', 'log-sig'},' trainlm}.

4.2.3. Network Training. According to the algorithm flow in Figure 4, the initial network training times were set as 100 times in parameter setting. The margin of error is set to 0.00001. The learning rate is set to 0.3. The simulated annealing algorithm was used to adjust the generation selection.

After the network is established, appropriate samples are determined according to the specific application and network size to train and learn network signals. This study establishes the characteristics and value range of evaluation indicators. 1500 samples were selected. After the normalization of the attribute values of each indicator. Partial data obtained are shown in Table 2.

Table 2: Sample data (part).

No.	Standardized economy feature	Standardized energy saving feature	Standardized environmental protection feature
1	0.1389	1	0.5832
2	0.2138	0.8201	0.8409
3	1	0.5106	0.4686
4	0.8511	0.6809	0.6395
5	0.7018	0.5328	0.7301
6	0.8202	1	0.7392
7	0.5457	1	1
8	0.2065	0.3540	0.6645
9	0.9708	1	0.6203
10	0.5145	0.5098	0.3642
11	1	0.6709	1
12	0.3955	0.3982	0.4084
13	0.7026	0.3453	0.8860
14	1	0.2529	1
15	0.8794	0.8135	0.8826

MATLAB was used to select 40 groups of samples in the sample set for network training. The maximum number of training cycles is 150. Then, the entire sample is tested. After repeated network training, it is found that the network tends to converge when the number of selected generations reaches about 30 times. The convergence effect is shown in Figure 6. The final error is 0.7461×10^{-5}.

4.2.4. Model Training Results. The RBF-BP neural network model is used to train the normalized data of three evaluation factors (economy feature, energy saving feature, and environmental protection feature). The curve of mean square deviation is shown in Figure 7.

As can be seen from Figure 7, BP neural network achieves convergence after about 54 times of iterations. However, RBF-BP neural network model needs about 28 times to achieve convergence. It can be seen that RBF-BP neural network improves the convergence speed and the mean square error is always lower than BP neural network, indicating that RBF-BP neural network can improve the accuracy of the model.

Figure 8 shows that although BP has a high evaluation accuracy (always higher than 80%), the evaluation accuracy of RBF-BP neural network is better than that of BP neural network. Statistical results show that in 40 groups of test data, the accuracy of training results of RBF-BP neural network model is greater than 90% and the accuracy of 22 groups was greater than 92%. This shows that the model has high approximation accuracy.

4.2.5. Solution of Index Weight. The results of neural network training only reflect the correlation between each neuron in the neural network. If it wants to get the weight of

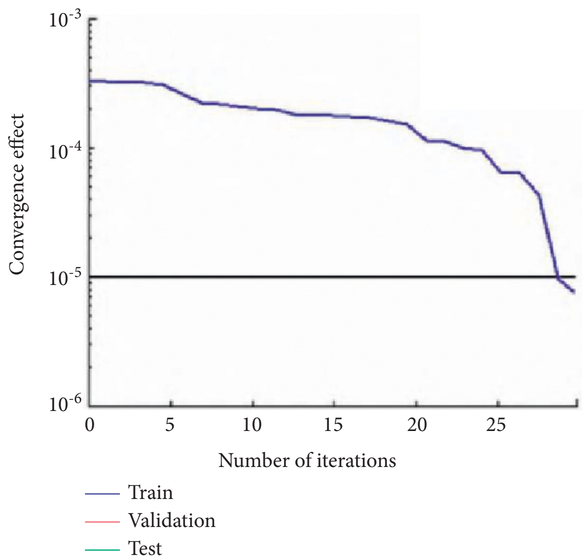

Figure 6: Network convergence.

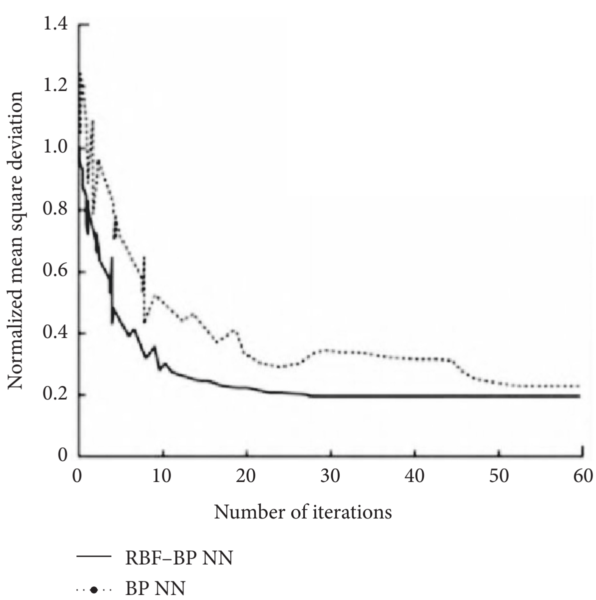

Figure 7: Normalized mean square deviation. The training accuracy of 40 groups of test samples is shown in Figure 8.

input factor to output factor, it needs to further analyze and process the weight of each neuron. In this paper, the following coefficients and indices are used to describe the relationship between input factor and output factor.

The relevant significant coefficient is

$$r_{ij} = \sum_{k=i}^{p} w_{ki} \frac{\left(1 - e^{-x}\right)}{\left(1 + e^{-x}\right)}, \tag{17}$$

$$x = W_{jk}, \tag{18}$$

The relevant index is

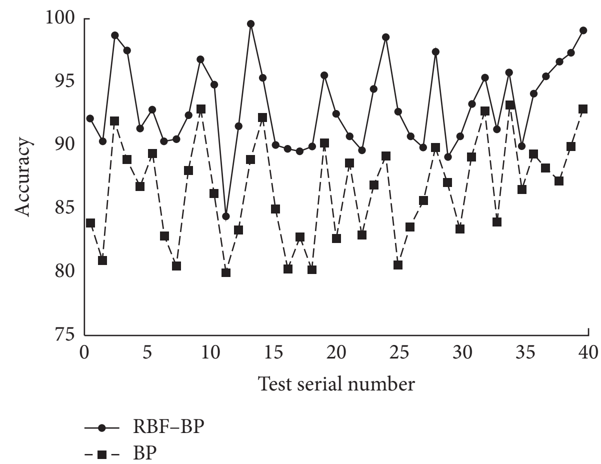

Figure 8: Training accuracy.

Table 3: Evaluation factor weight.

Evaluation factor	Weight
Economy feature	0.3082
Energy saving feature	0.3761
Environmental protection feature	0.3157

$$R_{ij} = \left| \frac{\left(1 - e^{-y}\right)}{\left(1 + e^{-y}\right)} \right|, \tag{19}$$

$$y = r_{ij}. \tag{20}$$

The absolute influence coefficient is

$$S_{ij} = \frac{R_{ij}}{\sum_{i=1}^{m} R_{ij}}, \tag{21}$$

where i is the RBF-BP neural network input unit, $i = 1\ldots, m$. K is the hidden unit of neural network, $k = 1\ldots, p$. J is the output unit of neural network, $j = 1\ldots, n$. w_{ki} is the weight between input layer neuron I and hidden layer neuron K. w_{jk} is the same weight of output layer neuron and hidden layer neuron k.

Among the above three correlation coefficients, the absolute influence coefficient s_{ij} represents the weight of input layer neuron I to output layer neuron J.

Using equations (17)–(21), the weight of each evaluation index is concluded, as shown in Table 3.

4.2.6. Construction and Application of the Investment Potential Model. We will use TOPSIS method to comprehensively evaluate the investment potential of different operation modes. By substituting the index data into TOPSIS model for calculation, the Euclidean distance and investment potential analysis values of different operation modes can be obtained, as shown in Table 4.

According to the investment potential analysis results, the investment potential analysis value of EPC mode is 0.9122, which is the best operation mode, and the investment potential analysis value of BOT mode is 0.8076, which is second only to EPC mode. The comprehensive benefit value of PPP mode is the lowest, 0.4231.

Table 4: The Euclidean distance and investment potential analysis values of different operation modes.

	Euclidean distance to the best point	Euclidean distance to the worst point	Investment potential analysis value
EPC	0.1250	0.0143	0.9122
BOT	0.0944	0.0243	0.8076
PPP	0.0882	0.1451	0.4231

5. Conclusions

The integrated energy project can realize the organic integration and collaborative optimization among electricity, heat, gas, water, and other energy sources, mainly by using the coupling and complementarity of various energy sources in time and space. It can coordinate the energy supply and demand, effectively improve the utilization rate of renewable energy, and reduce the use of fossil energy as much as possible. It can also achieve the cascade use of energy and improve the comprehensive energy efficiency on the user side and supply side. Under the background of energy conservation and emission reduction and large-scale promotion of electric energy substitution, fully exploring the complementary potential of various energy systems and realizing the optimization of comprehensive energy utilization are the most critical development goals of the current energy system. The key means to achieve the above objectives is to improve environmental benefits, energy consumption, economic cost, and other factors through an integrated energy project.

An investment potential analysis model of integrated energy project based on deep learning neural network is designed. The case study results show that the analysis results are roughly consistent with the actual conditions. At the same time, it also shows that the model has high yield, fast learning speed, high fitting accuracy, and stronger generalization ability and can accurately and scientifically analyze the investment potential of integrated energy projects. RBF-BP neural network can combine the fast convergence speed and good stability of RBFNN with the strong reverse self-study ability and generalization ability of BPNN. The correlation training model of each factor based on RBF-BP neural network algorithm reflects the complex nonlinear relationship of each factor in the comprehensive evaluation results in the investment potential analysis of integrated energy projects. It can automatically adjust the correlation weight according to the influence of each index on the investment potential, abandon the subjective influence caused by artificial weight, and have good generalization ability. RBF-BP neural network can carry out nonlinear mapping of any continuous function and more accurately reflect the relationship between evaluation indexes and evaluation results.

Data Availability

The data used to support the findings of this study are available from the corresponding author upon reasonable request.

Conflicts of Interest

The authors declare that they have no conflicts of interest.

References

[1] D. Zhang, H. Zhu, H. Zhang, H. H. Goh, H. Liu, and T. Wu, “An optimized design of residential integrated energy system considering the power-to-gas technology with multi-functional characteristics,” *Energy*, vol. 238, no. January 1, 2022.

[2] W. He, H. Lu, Y. Liu, G. Chen, and Z. Huang, “Rapid identification of economic indicators of integrated energy systems based on data analysis,” *Mathematical Problems in Engineering*, vol. 2022, Article ID 9180774, 13 pages, 2022.

[3] R Dhaya, U. J Ujwal, T Sharma et al., “Energy-efficient resource allocation and migration in private cloud data centre,” *Wireless Communications and Mobile Computing*, vol. 2022, Article ID 3174716, 13 pages, 2022.

[4] C. Yang, T. Hua, Y. Dai, G. Liu, X. Huang, and D. Zhang, “dongdong. Disturbance-Observer-Based adaptive fuzzy control for islanded distributed energy resource systems,” *Mathematical Problems in Engineering*, vol. 2022, Article ID 1527705, 12 pages, 2022.

[5] Z. Hu and L. Zhou, “A data-driven approach for electric energy equipment using wireless sensing technology in the context of carbon neutrality,” *Journal of Sensors*, vol. 2022, Article ID 3683723, 11 pages, 2022.

[6] S. Mohseni, A. C. Brent, S. Kelly, and W. N. Browne, “Demand response-integrated investment and operational planning of renewable and sustainable energy systems considering forecast uncertainties: a systematic review,” *Renewable and Sustainable Energy Reviews*, vol. 158, April 2022.

[7] K. Ökten and B. Kurşun, “Thermo-economic assessment of a thermally integrated pumped thermal energy storage (TI-PTES) system combined with an absorption refrigeration cycle driven by low-grade heat source,” *Journal of Energy Storage*, vol. 51, July 2022.

[8] L. Li, B. Lei, and C. Mao, “Digital twin in smart manufacturing,” *Journal of Industrial Information Integration*, vol. 26, no. 9, Article ID 100289, 2022.

[9] L. Li, T. Qu, Y. Liu et al., “Sustainability assessment of intelligent manufacturing supported by digital twin,” *IEEE Access*, vol. 8, pp. 174988–175008, 2020.

[10] L. Li and C. Mao, “Big data supported PSS evaluation decision in service-oriented manufacturing,” *IEEE Access*, vol. 8, no. 99, p. 1, 2020.

[11] L. Li, C. Mao, H. Sun, Y. Yuan, and B. Lei, “Digital twin driven green performance evaluation methodology of intelligent manufacturing: hybrid model based on fuzzy rough-sets AHP, multistage weight synthesis, and PROMETHEE II,” *Complexity*, vol. 2020, no. 6, pp. 1–24, Article ID 3853925, 2020.

[12] Y. Hu, J. Li, M. Hong, J. Ren, and Yi Man, “Industrial artificial intelligence based energy management system: integrated framework for electricity load forecasting and fault prediction,” *Energy*, vol. 244, no. April 1, 2022.

[13] F Alassery, A Alzahrani, A.I Khan, K Irshad, and S Islam, “An artificial intelligence-based solar radiation prophesy model for green energy utilization in energy management system,” *Sustainable Energy Technologies and Assessments*, vol. 52, August 2022.

[14] S. Sezer, F. Kartal, and U. . Özveren, “Artificial intelligence approach in gasification integrated solid oxide fuel cell cycle,” *Fuel*, vol. 311, 2022.

[15] F. Khosrojerdi, O. Akhigbe, S. Gagnon, A. Ramirez, and G. Richards, “Integrating artificial intelligence and analytics in smart grids: a systematic literature review,” *International Journal of Energy Sector Management*, vol. 16, no. 2, pp. 318–338, 2022.

[16] K. B. Letaief, Y. Shi, J. Lu, and J.. Lu, “Edge artificial intelligence for 6G: vision, enabling technologies, and applications,” *IEEE Journal on Selected Areas in Communications*, vol. 40, no. n 1, pp. 5–36, 2022.

[17] S. Zheng, R. Yuan, L. Zhou, X. Yang, and H. Xiong, “Data security aggregation method of smart grid based on BP neural network,” *Energy Systems*, vol. 20, 2022.

[18] B. Chen and Y. Wang, “Short-term electric load forecasting of integrated energy system considering nonlinear synergy between different loads,” *IEEE Access*, vol. 9, pp. 43562–43573, 2021.

[19] F. Wu, R. Jing, X.-P. Zhang, F. Wang, and Y. Bao, “A combined method of improved grey BP neural network and MEEMD-ARIMA for day-ahead wave energy forecast,” *IEEE Transactions on Sustainable Energy*, vol. 12, no. 4, pp. 2404–2412, October 2021.

[20] G. Liu, “A new method for fault diagnosis of building electrical system based on rbf-bp neural network,” in *Proceedings of the - 2019 International Conference on Intelligent Computing, Automation and Systems, ICICAS*, pp. 470–474, Chongqing, China, December 2019.

[21] B. Ma, Y. Zhang, and L. Ma, “Research on the formation mechanism of MgO and Al2O3on composite calcium ferrite based on DA-RBF neural network,” *Computational Intelligence and Neuroscience*, vol. 2022, Article ID 4327969, 12 pages, 2022.

[22] N. Liu, J. Zhang, S. Zhao, J. Xu, and Y. Wang, “A novel MPPT method based on large variance GA-RBF-BP,” in *Proceedings of the 2017 Chinese Automation Congress*, Jinan, China, October 2017.

[23] X. Li, T. Zhang, Z. Deng, and J. Wang, “A recognition method of plate shape defect based on RBF-BP neural network optimized by genetic algorithm,” in *Proceedings of the 26th Chinese Control and Decision Conference*, Changsha, China, June 2014.

[24] H. Wen, W. Xie, J. Pei, and L. Guan, “An incremental learning algorithm for the hybrid RBF-BP network classifier,” *EURASIP Journal on Applied Signal Processing*, vol. 15, 2016.

[25] H. Hu, Y. Song, Pu Fan, C. Diao, and N. Cai, “A backstepping controller with the RBF neural network for folding-boom aerial work platform,” *Complexity*, vol. 2022, Article ID 4289111, 9 pages, 2022.

[26] S. Zhang and C. Duan, “Clustering optimization algorithm for data mining based on artificial intelligence neural network,” *Wireless Communications and Mobile Computing*, vol. 2022, Article ID 1304951, 16 pages, 2022.